SEISMICITY, ACTIVE STRESS PATTERN AND FAULT REACTIVATION POTENTIAL IN SOUTH CARPATHIANS

E. OROS, A. O. PLACINTA, I. A. MOLDOVAN

National Institute for Earth Physics, 12 Calugareni Street, Magurele 077125, Ilfov District, Romania,
E-mail: anca@infp.ro

Received June 7, 2021

Abstract: The paper presents a seismotectonic model of the Southern Carpathians obtained from the analysis of the seismicity-stress field-geology and tectonics relationship. The seismicity model is based on a revised earthquake catalogue. The distribution of b-values in the 3D space facilitated the identification of stressed areas and asperities with reactivation potential and their correlation with geological structures. The stress field has been modelled using the parameters of the stress tensor calculated by the formal inversion of the focal mechanisms. The reactivation potential of geological structures was estimated depending on the relationship between the fault planes geometry and the principal stress axes.

Key words: seismicity, active stress, recurrence period.

1. INTRODUCTION

In the space of the Southern Carpathians, [1] defined two important seismogenic zones, respectively the *Danube Seismogenic Zone* (DSZ), in the West and the *Fagaras-Campulung Seismogenic Zone* (FCSZ), in the East (Figure 1).

Recent seismicity studies made by [2, 3, 4, 5] highlighted, in the central part of the investigated orogen, several areas with important seismic activity (Mw > 5.0), defined as the *Central-South Carpathian Seismogenic Zone* (CSCSZ) with significant impact on the seismic hazard of Romania. The seismicity of the Southern Carpathians is grouped mainly at their contact with the Pannonian, Transylvanian and Getic Depressions, generally at the intersection of the faults that controlled the evolution of some neotectonic structures, like depressions and grabens.

The strongest earthquakes were registered in the area of Moldova Noua (10.10.1879, Mw = 5.8) after [3], in Caransebes-Mehadia Depression (18.07.1991, Mw = 5.7), in Hateg Depression, on the South Carpathian Fault (09.07.1912, Mw = 5.2, after [3]), and in Brezoi-Titesti Depression, at the intersection of the Intra-Moesica with the South-Carpathian Faults (16.01.1916, Mw = 6.4).

Recent studies have associated seismicity with geological structures reactivated in a compressive NW–SE stress field in the East and extensional NE–SW in the West (*e.g.* [1, 3, 5–10]).

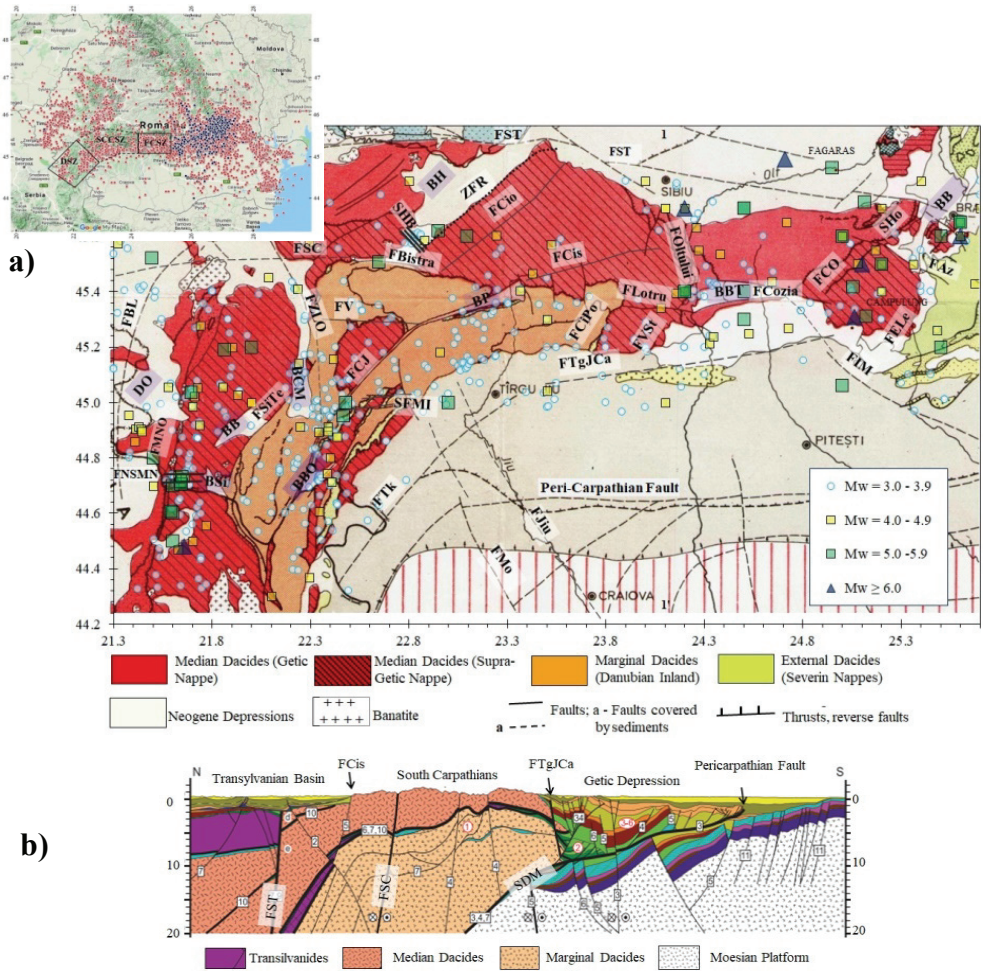

Fig. 1 – (Color online) a) Seismological and tectonic features of the South Carpathians [11, 12]. Seismicity after [13, 14] and this study. b) Profile 1-1'.

This paper shows an assessment of the seismogenic potential of geological structures in the Southern Carpathians, based on a detailed analysis of the causal relationship between seismicity, contemporary stress field and crustal tectonics. An important achievement of the paper is the estimation of the probability of reactivation of fault systems (slip tendency) and the associated maximum possible magnitude and recurrence period.

2. GEOLOGICAL, GEOPHYSICAL AND TECTONIC FEATURES

The Southern Carpathians are made up of a succession of pre-Alpine and Alpine nappes (Dacides and Transylvanides) covered locally by post-tectonic and Neogene sediments (Fig. 1a) [11]. At the crustal level, several systems of longitudinal, transversal and oblique faults are known to the orientation of the mountain range, which controlled the formation of Neogene basins of the pull-apart type. The South-Carpathian Fault (FSC), with the segments Bistra, Lotru and Cozia intersect with the Intramoesica Fault (FIM) on the Eastern flank of the Brezoi-Titesti Basin dividing the Southern Carpathians into two structural sectors. Each sector is fragmented into tectonic blocks bordered by generally vertical and preferentially oriented faults NNW-SSE to NNE-SSW and Neogene structures [12] (Figs. 1a, 1b and Fig. 2). The epicenters represented in Fig. 1 are taken after Romplus (www.infp.ro): depth $h < 50$ km red circles; $h > 50$ km blue circles. Polygons in the map from the upper left corner of Fig. 1a define the seismogenic zones: Danube, (DSZ); Fagaras-Campulung, (FCSZ) after [1] and Central-South Carpathians, (CSCSZ). Tectonics and geotectonic data are taken from [11, 12, 15, 16].

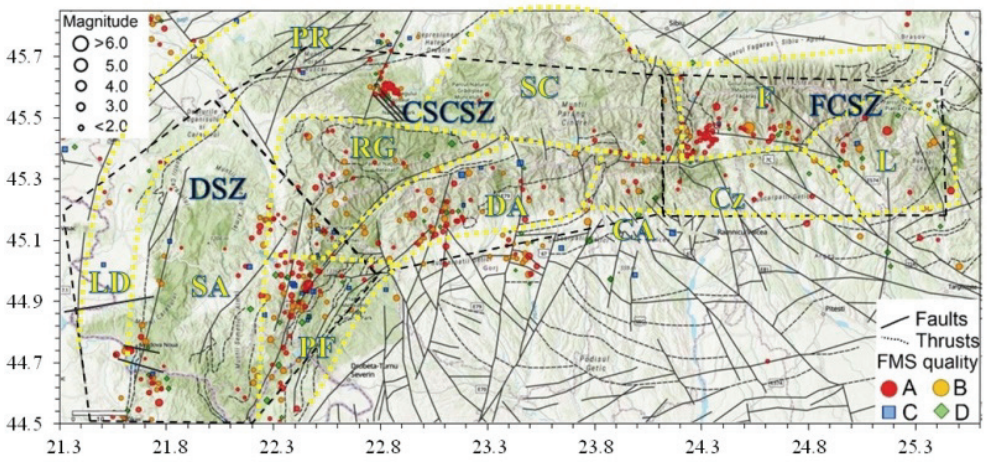

Fig. 2 – (Color online) Distribution of earthquakes with focal mechanisms (quality A, B, C and D); broken black lines delimit seismogenic areas; the dotted yellow lines delimit the tectonic blocks defined by [16]: DL, Dognecea-Locva; SA, Semenic-Almaj, PF, Iron Gates, RG, Retezat-Godeanu; PR, Poiana Rusca; DA, Danubian; SC, Sebes-Cibin; F, Fagaras, Ca, Capatana, Cz, Cozia; L, Leaota.

On the main map of Fig. 1a are also marked the following units: (i) Intra-mountain depressions: DO, Oravita; Bsi, Sichevita; BCM, Caransebes-Mehadia; BBO, Bahna-Orsova; BP, Petrosani; BBT, Brezoi-Titesti; BB, Brasov; (ii) Faults: FST, South-Transylvanian; FSC, South-Carpathian with its main segments (Bistra, Lotru, and Cozia); ZFR, Shear Zone Rasinari; FBL, Bazias-Lugoj; FNSMN, North

and South Moldova Noua faults; FZLO, Zarand-Lugoj-Orsova; FMNO, Moldova Noua-Oravita; FsiTe, Sichevita-Teregova; FCJ, Cerna-Jiu; FTk, Timok; SFMI, Mehadia-Isverna (Baia-de-Arama system); FV, Virciorova; SHB, Hateg-Bistra system; FCio, Cioclovina; FCis, Cisnadie; FtgJCa, Tg. Jiu-Calimanesti; FMo, Motru; FJiu, Jiu; SDM, Danubian-Moesian system; FciPo, Ciungesti-Polovraci; FVSt, Valea lui Stan; FCO, Curmatura Oticului; SHo, Holbav thrust; FELe, Est-Leaota; FIM, IntraMoesica; Faz, Azuga. In Figure 1b, on the Profile 1-1' taken after [17] are represented FST, South-Transylvanian Fault; FSC, South-Carpathian Fault; FTgJCa, Tg. Jiu-Calimanesti Fault.

The Northern sector of FSC is relatively compact with three large tectonic blocks (Poiana Rusca, Sebes-Cibin and Fagaras), compared to the southern sector, which consists of several smaller tectonic blocks (Locva-Dognecea, Semenic-Almaj, Retezat-Godeau, Iron Gates, Danubian, Capatana, Cozia and Leaota). The South Transylvanian (FST) and Bazias-Lugoj (FBL) faults are the tectonic contacts between the orogen with Transylvanian and Pannonian Depressions. The contact with the Moesic Platform consists of a fault system parallel to the Timok (FTk) and Targu Jiu-Calimanesti (FtgJCa) faults that intersect the Pericarpathian Fault forming the *Danube-Moesian System* (SDM) (Fig. 1b).

Although data on the evolution of the stress field over time and the kinematic evolution of the Southern Carpathians are contradictory [18], two major events with brittle deformations can be noted ([19] and references included). The NE-ENE contractions with lateral-right transcurrent faults from the Paleogene-Middle Miocene are replaced in the Middle Miocene-Pliocene with NW–SE compression and lateral-right transcurrent faults on ESE-oriented structures (FSC system) in transtensive tectonic regime in the West (FBistra), pure strike-slip in the centre (FLotru) and compressive in the East (FCozia). During this period, the FSC, FCJ and FSiTe, SHB, SFMI and FTk faults favoured the formation of the Hateg, Vidra, Petrosani, Sichevita, Bozovici, Caransebes-Mehadia pull-apart basins, and the Getic foreland is divided up through a system of lateral-right faults (FTgJCa and SDM). In the Pleistocene-Holocene, the E-W extension is contemporary with the ESE–WNW contraction in the Vrancea area. The contemporary stress field is extensive, heterogeneous, with maximum horizontal stress (SHmax) oriented NW–SE in the West and NE–SW in the East [7, 20].

Geodetic models of recent crustal deformations are characterized by velocity vectors, oriented S and SE in the west of the region, SSW to SW in the East and West in the centre [21, 22]. Recent positive and negative vertical movements are strongly contrasting between different tectonic blocks [23, 24, 25]. Thus, the Leaota Block rises by +5 mm/year at the intersection of FIM and FCozia. The velocity decreases suddenly to 1–2 mm/year in the Fagaras Block, at the intersection of the FOlt with FCozia and maintains up to the Petrosani Basin where it becomes accentuated negative of –2 mm/year [25].

The Dognecea-Locva and Semenic-Almaj blocks rise by +2 mm/year in contrast to Orsova Depression (–2 mm/year) and the Godeanu-Retezat block (0 mm/year). Contextually, FIM, FCozia, FCO, Sho, FELe, FCJ, FBistra, FZLO, FMNO, and FBL appear as geologically active, as areas with stress accumulations.

3. DATA AND METHODS

Our study is based on a *Parametric Earthquake Catalog* (PEC) and a *Focal Mechanisms Catalogue* (FMC), both catalogues revised and updated on 31.12.2020. The PEC is a compilation based on the catalogues developed by [3, 8] and the Romplus catalogue [13]. The earthquakes of 1900–1979 were relocated by the grid-search technique using the Seisan program [26], the IASPEI91 velocity model and many data obtained from digitized analogue seismograms and seismic bulletins collected through EuroSeismos (http://storing.ingv.it/es_web) and Sismos-Neries 2006–2010 projects (http://seismogramrequest.rm.ingv.it). The moment magnitude, Mw was calculated according to the available data applying: i) the conversion relations Mw = f (Io; Ri; Mi) elaborated by [3, 27] when the maximum intensity (Io/max), radii of isoseists (Ri), macroseismic and instrumental magnitudes (Mi) are available, ii) the relation (1) of [28] calibrated by [3] and iii) the scalar moment method using the relations (2) and (3).

$$\log Mo = \log (A_\omega/V_\omega) - \log T_\Delta + 1.66 \log \Delta + K \quad (1)$$

where A_ω = maximum amplitude at the period Tω at which the instrument has the amplification V_ω, T_Δ = the period at the distance Δ (km), K = 15.49 (coefficient calculated by [3]).

$$Mo = 4\,\pi\, DE\, v3\rho\, OM/G\,(r, h)\, KK \quad (2)$$

$$w = 2/3 \log Mo - a \quad (3)$$

where ρ = density, v = seismic wave velocity at source depth (P or S), DE epicentral distance, OM = displacement spectrum plateau corrected with attenuation, KK = attenuation factor, G (r, h) = radius parameter, a = 6.06 for Mo in Nm; a = 10.73 for Mo in dynes-cm.

The PEC contains 521 events produced between 09.06.1523 and 31.12.1989. Of these, 410 events with Mw ≥ 3.0 were revised. The macroseismic revision, based on intensities in *individual observation points* (IDP), maximum intensities (Imax/Io) and or isoseist rays (Ri), was performed using methods and mathematical relations instrumentally calibrated at the regional level by [27, 29, 30]. The locations obtained

with the MEEP method ([31]) were validated by comparative analysis with those calculated using the Bakun-Wentworth, BKW method [32]. The depth of the foci was calculated with Blake's relation [29]. Mw calculated with MEEP / BKW were validated by comparison with those calculated with the relations Mw = f (Io/max; Ri) [27]. When the macroseismic data were insufficient, we used the fixed value depth equal to the average calculated from recent data (h = 13.6 ± 6.9 km). The initial compilation, with 7578 events (Mw = 0.1 – 6.6, h = 0.4 – 50.0 km) (Fig. 1a, inset) was decontaminated, the possible explosion events being eliminated by the method of the ratio between the number of events produced per day (07–15 hours) and those produced at night, but after careful analysis of explosion-specific seismograms (*e.g.* monochrome spectrograms, Rayleigh wave domination, positive polarity for the P phase on the vertical component at all stations, repeatability of events in the same area at the same time of day).

After decontamination, the PEC contains 1970 earthquakes (Mw = 2.6 = 6.6, h = 0.5–50 km) (Fig. 1a). Were identified and parameterized 132 new earthquakes, N = 50 events with macroseismic parameters and N = 82 with instrumental parameters. Table 1 presents all revised events with Mw ≥ 5.0. We identified false earthquakes in the Romplus catalogue which are points of macroseismic observation for strong earthquakes produced in neighbouring countries (Table 2). For example, for the earthquake of March 24, 1922, the new instrumental location is in Serbia, but in Romplus it is located at Berzovia (450/220) with Io = VI^0MSK and Mw = 4.1. For the epicentral distance De = 142 km to Berzovia calculated with the new epicenter results the intensity, Io = IX^0MSK, Ms = 6.0 [33] and h_instr = 18.9 km we obtain intensity I = V–VI^0MSK. For the Timisoara location (De = 112 km) results Ii computed = V–VI^0MSK, a value comparable to that in his catalogue [14] where Iobs = V^0MSK. The same result is obtained for the earthquake of 12.08.1924 located at the border of Serbia / Hungary / Croatia. The earthquakes of 04.05.1963 and 09.07.1912, initially located in the Tg. Jiu area, have the revised epicentres in the Hateg area, with h = 19.6 km and Mw = 5.0 and h = 34.1 km and Mw = 5.2, respectively.

The catalogue of focal mechanisms, FMC is the one obtained by [9, 20] which we updated on 31.12.2020. It contains 469 quality A and B mechanisms (Mw = 1.2 – 6.6, h = 1.0 – 57.0 km) distributed in all seismically active areas (Fig. 2). The focal mechanisms were calculated using the HASH method [34, 35] based on the P waves polarities and S/P amplitude ratios.

The distribution in 3D space of the b values in the Gutenberg-Richter relation (relation 4), obtained with the Zmap program [36], reflects the stress state in the crust, between b and the differential stress (σ1–σ3) there is the relation (5) [37]. The stress field was modelled and studied using the distribution of stress tensor parameters determined by the formal inversion of quality focal mechanisms A and B (data set with Nmin = 30 mechanisms) (Fig. 2).

Table 1

Macroseismic parameters for earthquakes with Mw ≥ 5.0

Nr.	Year	Month	Day	Hour	Minute	Lat N	err (km)	Long E	err (km)	h (km)	err (km)	Mw	±σ
1	1523	6	9	x	x	45.600	50	25.800	50	12.2	7.8*	5.9	0.4
2	1545	7	9	8	30	45.600	50	25.600	50	21.4	–	6.2	0.4
3	1550	10	26	1	x	45.700	20	24.200	20	12.3	6.9*	6.1	0.4
4	1569	8	17	5	x	45.400	50	24.500	50	15.8	2.3	5.9	0.4
5	1571	4	10	7	x	45.700	50	24.500	50	12.3	6.9*	5.6	0.4
6	1639	4	9	1	x	45.400	50	24.200	50	13.7	7.3*	5.2	0.4
7	1665	1	19	x	x	45.507	50	22.647	50	13.7	7.3*	5.0	0.4
8	1793	12	8	5	x	45.419	56	25.054	56	24.0	8.6	5.8	0.3
9	1826	10	16	1	x	45.700	10	24.500	10	23.2	–	5.2	0.4
10	1832	2	19	7	8	45.300	20	24.500	20	16.4	3.2	5.9	0.4
11	1879	9	28	15	30	44.800	10	21.500	10	12.0	4.2*	5.1	0.4
12	1879	10	10	15	45	44.733	3.8	21.647	3.8	15.8	7.2	5.8	0.1
13	1879	10	11	2	45	44.704	7.4	21.641	7.4	12.7	5.6	5.3	0.1
14	1879	10	20	10	45	44.716	1.4	21.637	1.4	13.2	1.9	5.2	0.1
15	1880	2	23	21	30	44.500	40	21.600	40	12.0	4.2*	5.1	0.4
16	1880	3	1	2	45	44.700	10	21.600	10	12.0	4.2*	5.1	0.4
17	1880	4	13	12	20	44.600	10	21.600	10	12.0	4.2*	5.1	0.4
18	1894	12	19	22	33	45.037	2.0	21.694	2.0	13.2	7.0	5.3	0.4
19	1909	8	31	21	21	45.190	14.9	21.862	14.9	22.7	7.6	5.2	0.2
20	1910	10	11	11	54	45.001	15.9	22.479	15.3	16.2	9.6	5.2	0.1
21	1912	7	9	21	46	45.592	52.5	22.894	52.5	34.1	8.9	5.2	0.4
22	1916	1	26	7	38	45.307	15.1	25.061	17.9	18.4	5.9	6.6	0.2
23	1916	1	26	8	30	45.400	20	24.200	20	13.7	7.3*	5.2	0.4
24	1919	4	18	6	20	45.724	44.5	25.115	44.5	35.0	7.3	5.6	0.4
25	1927	5	31	22	58	44.607	29.8	21.591	28.5	22.4	20.0	5.2	0.4
26	1943	6	20	1	0	45.000	10	23.000	10	13.7	7.3*	5.2	0.4
27	1963	5	4	16	48	45.599	5.3	23.094	3.8	19.6	5.9	5.0	0.4
28	1966	6	10	9	12	45.061	4.1	25.000	4.1	33.3	7.4	5.0	0.4
29	1969	4	12	20	38	45.310	10	25.120	10	26.7	–	5.4	0.2
									New events				
1	1571	5	19	18	x	45.650	50	25.600	50	13.1	9.5	5.2	0.4
2	1571	5	25	0	x	45.600	50	25.000	50	21.2	–	5.4	0.4
3	1599	12	11	x	x	45.650	50	25.600	50	12.2	7.8	5.1	0.4
4	1605	12	24	x	x	45.500	20	25.100	20	21.1	3.9	6.4	0.4
5	1606	1	13	1	x	45.500	20	25.200	20	16.2	–	5.4	0.4
6	1739	2	4	0	0	44.000	40	21.300	40	12.0	4.2*	6.4	0.5
7	1862	10	16	1	11	45.600	22	25.500	22	18.5	5.8	5.0	0.4
8	1864	12	4	1	3	45.200	5	22.000	5	23.8	8.8	5.0	0.4
9	1893	4	8	13	47	44.480	20	21.660	20	14.7	6.1	6.3	0.4
10	1932	5	27	10	42	45.200	31	25.500	31	21.9	–	5.2	0.4

* focal depth computed on digital data basis for regional morfo-structures; 50 km are the latitude and longitude estimated errors, on singular macroseismic data having only informal significance about large uncertainty of location; depth without error is computed from Io, Mw, h instrumental.

Table 2

Instrumental parameters of earthquakes recorded between 1900 and 1980

Date ddmmyyyy	Time hhmmss.s	err (sec)	latN (O)	err (km)	longE (O)	err (km)	h (km)	err (km)	Nst	rms (sec)	gap (O)	Mw	Ref.
31081909	212227.0	1.9	45.188	27.0	21.862	18.4	14.0	F.F	3	1.30	305	5.1±0.2	#
	212129.0		45.100		21.800		20.0					4.4	Ro
11101910	115403.3	1.4	45.001	15.9	22.479	15.3	16.2	9.6	6	1.36	260	5.2±0.1	#
	115209.0		44.900		22.400		7.0					4.5	Ro
26011916	073803.7	6.30	45.307	15.1	25.061	17.9	18.4	5.9	23	4.1	147	6.6s	#
	073810.4	0.79	45.212	3.5	25.370	4.5	15.7	3.3	8	0.3	162	6.4	O08
	073754.0		45.400		24.600		21.0					6.4	Ro
24031922	122206.1	8.1	45.028	16.4	20.192	25.9	18.9	22.4	28	4.8	111	6.4s,Imax	#
	122150.0		45.000		22.000		9.9					4.1	Ro
12081924	162740.0	5.6	46.256	11.9	18.940	20.3	20.0	21.0	12	3.8	146	5.4s,Imax	#
	162737.0		45.000		22.000		9.9					–	Ro
31051927	225831.8	1.9	44.709	11.8	21.585	12.1	11.7	9.4	17	2.1	234	5.2B±0.4	#
	225815.0		44.900		21.700		16.0					4.4	Ro

rms = average square root, gap = azimuthal deficit of the location; F.F. = fixed depth value; Ref = bibliographic references; # = [41]; Mw = moment magnitude calculated with the scalar moment method or s, Io-Mw = f (Ms; Imax); B = Mw calculated from the amplitudes of the waves with its relation [28]; O08 = [40], Ro = Romplus catalog www.infp.ro.

$$\log N = a + bM \tag{4}$$

$$b = 1.2 \pm 0.06 - 0.0012 \pm 0.0003\ (\sigma 1 - \sigma 3) \tag{5}$$

The inversion was performed with Zmap [36] and WinTensor [38]. The parameters of the stress tensor are the main axes (σ1-compression > σ2-null > σ3-extension), the relative magnitude of the stress (R = σ1 – σ2 / σ1 – σ3) with values R = 0 – 1, the horizontal stresses SHmax and Shmin and the tectonic regime index R' with values R' = 0.0 – 3.0. R' was calculated according to the plunge angles of the main axes, respectively R' = R when σ1 is vertical (extensive stress regime), R' = 2 – R when σ2 is vertical (compressive stress regime with sliding on the direction fault), R' = 2 + R, when σ3 is vertical (compressive stress regime with inverse faults). The inversion is performed assuming that the crustal stress is uniform, the earthquakes are independent and occur on faults with various directions and the slip vector is in the direction of the shear stress. For each fault, the probability of reactivation (slip tendency, ST) was calculated. The ST is defined by the ratio between the shear and normal stress, the slip being possible when this ratio exceeds the friction coefficient on the fault surface [39]. The results obtained are given in Table 3.

The coefficients a and b in relation 4 are used to calculate the probabilistic hazard with relation 6:

$$\mathrm{Tr}\ (\mathrm{Mw_x}) = 1/10^{\,a_{yearly} - b\mathrm{Mw}_x} \tag{6}$$

where Tr is the recurrence period (years) of events with M ≥ Mwx. The results obtained are given in Table 4.

Table 3

The results of the stress tensor inversion. S_i = the main axes of the tensor, R = the relative magnitude of the tension, R '= the index of the tension regime, RTT = the regime of the tectonic tension

Zone sub-zone	Nr. MF	σ1 (^{0}) az/plunge	σ2 (^{0}) az/plunge	σ3 (^{0}) az/plunge	R	R'	SH_{max} (^{0})	Sh_{min} (^{0})	RTT*
DSZ	139	328/74±19.7	103/12±52.4	196/11±49.0	0.09	0.09±0.13	124±47	34	REx
Mehadia	49	285/69±9.7	181/5±26.8	89/20±26.4	0.08	0.08±0.07	121±39	31	REx
Moldova Noua	14	302/51±5.6	100/37±15.0	199/11±15.4	0.18	0.18±0.09	117±8	27	REx
FCSZ	127	243/56±27.9	71/34±40	339/4 ±36.4	0.20	0.2±0.18	66±34	156	REx
Brezoi – V. Oltului	43	204/50±31.9	38/39±32.4	302/7±10.2	0.86	0.87±0.26	32±7	122	SSE
Titesti-Brezoi Basin	20	243/31±26.5	70/59±26.5	337/2±3.8	0.96	1.04±0.04	66±3	156	ESS
NV Campulung	14	110/22±20.4	262/65±24.7	16/11±14.8	0.33	1.67±0.18	108±5	18	PSS
SE Campulung	17	160/12±22.2	18/75±26.5	253/9±23.1	0.41	1.59±0.35	161±14	71	PSS
CSCSZ	144	285/59±17.7	84/29±37.6	180/8±35.5	0.13	0.13±0.15	101±21	11	Rex
Hateg Basin	86	308/65±53	93/21±53.2	188/13±9.1	0.99	0.99±0.20	98±7	9	ESS
RG Block	21	254/75±36.1	78/15±36.4	348/1±8.8	0.45	0.45±0.29	78±9	168	PEx
NV Tg. Jiu	36	279/5817.9	92/31±33.3	184/3±29.2	0.15	0.15±0.13	97±19	7	REx
Tirgu Jiu	18	33/4±14	295/65±58.8	125/25±58.1	0.09	2.22±0.23	33±3	123	CSS

NrMF = number of focal mechanisms, * Stress regime [38]: Rex = radial extension. (R'=0–0.25, σ1 vertical), PEx = pure extension (R'=0.25–0.75, σ1 vertical), ESS/SSE = transtensiv (R'=0.75–1.0, σ1 vertical/R'=1.0 – 1.25, σ2 vertical), PSS=pure strike-slip (R'=1.25–1.75, σ2 vertical), SSC/CSS=transpresive (R'=1.75–2.0, σ2 vertical/ R'=2.0–2.25, σ3 vertical), PC=pure compression (R'=2.25–2.75, σ3 vertical), RC=radial compression (R'=2.75–3.0, σ3 vertical).

Table 4

Seismotectonic characteristics of seismogenic sources in the Southern Carpathians

Source	Geological Structures/faults	Main faults (strike)	Reactivation potential (%)	M_{max}	a_{year}/b	$Tr(M_{max})$ (years)
DSZ	Moldova Noua-Oravita (FMNO, FBL)	– NNE–SSV (FMNO, FBL) – NV–SE, EV, ENE–VSV (Neogene basins, FNSMN)	15–20 90–95	6.2	1.95/ 0.69	212
	Mehadia (FCJ, FZLO, FMI,FSiTe, FV) and intersections	– NE–SV (FCJ, FSiTe) – NNE–SSV – NNV–ESE (FZLO, FCJ/South Mehadia) – E–V (FMI, FV)	40–60 75–80 >95	6.2	2.35/ 0.88	1275
FCSZ	Brezoi (FOltului, FLotru, FCozia, FVSt)	– NE–SV (FVSt) – ENE–VSV– E–V (FCozia, FLotru) – NS la NNV–SSE (FOltului)	90 85–90 40–60	6.9	1.03/ 0.55	582
	NV Campulung (FCozia, FIM, FCO)	– NE–SV (FCO) – EV (Cozia) – NV–SE (FIM)	30 80–90 95	6.9		582
	SE Campulung (FIM, FELe)	– NV–SE (FIM) – NNE–SSV (FELe)	95 40–60	6.9		582
CSCSZ	Bazinul Hateg (FBistra, FCio, ZFR, SHB)	– NE–SV (ZFR, FCio) – NV–SE – VNV–ESE (SHB) – EV (FBistra)	80 90 90–95	5.7	1.85/ 0.85	988
	Blocul Godeanu-Retezat (FCJ, FV)	– VNV–ESE (FV) – ENE–VSV (FCJ)	75–85 95	5.7		988
	NV Tg. Jiu (FJiu, FMo, SDM)	– NV–SE (FMo, FJiu) – EV – NE–SV (SDM)	75–80 90	5.7		988
	Tg. Jiu (FJiu, FTk, FTgJCa)	– NNV–SSE la NNE–SSV – ENE–VSV (FTk, FtgJCa)	95 25	5.7		988

4. RESULTS AND DISCUSSIONS

4.1. SEISMICITY

The spatial distribution of the epicentres (Fig. 1) shows a clear tendency to group the hypocenters of strong earthquakes on correlated alignments with tectonics, within the limits of location errors and uncertainties in geological data. So far, 39 earthquakes with Mw ≥ 5.0 are known. These can be causally associated with well-individualized faulted geological structures, respectively with: 1) the FMNO system (Moldova Noua and Oravita events) and the intersection of FZLO, FCJ and FMI (Mehadia events) in DSZ, 2) with the faults that controlled the Hateg Basin (ZFR, SHB and FCio) and the faults from the contact between Getic Depression and orogen in the CSCSZ, and 3) with the structure defined by the intersection FLotru-FCozia-FOltului (Fagaras/Bazinul Titesti-Brezoi events) and the intersection FCozia-FIM-FCO-SHo (Leaota-Bazovul Brasov events) in FCSZ (Fig. 1a). Earthquakes with Mw > 6.0 are known only in FCSZ at the intersections FST-FOltului and FIM-FCozia-SHo-FCO and in Serbia, South of the Danube, most likely on FMNO. The most important event, well documented macroseismic and instrumental by [40], occurred on 26.01.1916 (Mw = 6.6, h = 18 km, Io = VIII^{0}MSK) in FCSZ. Earthquakes with Mw = 3.0 – 4.9 follow in the same distribution, their groups more clearly defining active tectonics.

The distribution of focal depths highlights some seismotectonic differences between the three seismogenic areas. The seismic activity clusters at h = 12 km in DSZ, in a compact volume in CSCSZ (h = 2–18 km) and on 3 levels in FCSZ (h = 1–5 km, h = 10 km, h = 14 km). The average values of the coefficients a and b from the GR relation calculated for the whole Southern Carpathians, using the decontaminated catalogue, are b = 0.75 ± 0.16, a = 5.19 (annually = 2.5) with the magnitude of completeness Mc = 4.2 ± 0.23. The spatial distribution of b-values, determined in a grid with nodes spaced at $0.05^0 \times 0.05^0$ for N = 150 (Nmin = 25) events/node, shows a large variation of them suggesting a strong heterogeneity of the stress field at the level of the whole region (b = 0.4–1.4) (Fig. 3).

Due to incomplete data, the seismicity model (b-value distribution) is affected by uncertainty. Thus, at the contact between Sebes-Cibin Block and Fagaras Block, bordered to the South by Brezoi-Titesti Depression, a narrow area can be observed that divides the orogen into two distinct sectors. One in the West, with several areas characterized by a substantial increase in stress (b < 0.8) and the existence of areas of "asperities" (volumes with strongly contrasting values) that have a high potential for reactivation in the future. They are located on seismically active faults (Mw ≥ 5.0) at deep levels where strong earthquakes have occurred; example the Moldova Noua and Oravita areas where strong earthquakes occurred in 1879, 1894 and 1909, respectively, the Cerna-Timis Valley with the Mehadia epicentral zone (FCJ-FZLO-FMI intersection) where the events of 1910 (Mw = 5.2) and 1991 (Mw = 5.7) are known and Hateg Basin where, at the intersection of the FSC-SHB-ZFR-FCio faults, the major earthquakes of 1665, 1963 and 1912 were registered.

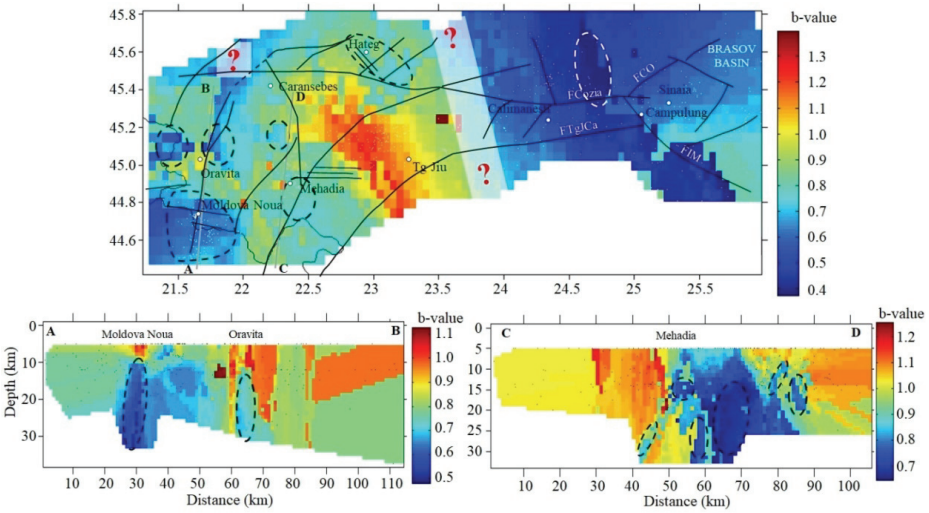

Fig. 3 – Spatial variation of b-value and A–B and C–D profiles from DSZ.
Ellipses are stress increase areas and asperities.

The distribution of deep asperities between Orsova and Northern Mehadia (Fig. 2, CD profile) is complex. Here, we notice one in the Orsova area from the depth interval 20–30 km, where recently (25.06.2020) occurred an earthquake with Mw = 4.1 at a depth of 22 km [8]. Also, in the north of the C–D profile, there are two asperities between 5–20 km depth where the seismic activity has known a recent intensification [4, 5]. The other sector, East of the orogen, shows a compact model of the distribution of b-values, with low values (b < 0.85) suggesting a stressed environment with areas of asperities along with the FIM, at the intersection with FCozia and FtgJCa, FCO where the 1916 earthquake occurred.

4.2. STRESS FIELD AND SEISMOTECTONIC FEATURES

The 2D model of the stress field (orientation of σ1 and the typology of active faults) from Fig. 4 was obtained using a grid with nodes spaced at $0.10^0 \times 0.10^0$ and N = 30 focal mechanisms for each node. There is a high level of heterogeneity of the stress field caused by the large variation of the orientation of the σ1 axis while the stress regime is constant, predominantly extensive. The σ1 axis shows a sinusoidal pattern, with successive rotations from NE–SW to NW–SE, both North and South of FSC. In detail, we can note a good correlation between the structure in blocks and the distribution of areas where the orientation of the σ1 axis remains unchanged.

The faults are predominantly normal or strike-slip with a large normal component, except for the contact area between the orogen and Getica Depression, where the faults are strike-slip in a regime of compressive stress, the only area with

b = 0.95–1.4. The extensive stress regime is best characterized by the orientation of the Shmin axis which is oriented approximately NNE-SSW in the western half of the orogen (DSZ and CSCSZ) and NW–SE in the East (FCSZ). In DSZ the σ1 axis rotates from NE–SW in the West to NV–SE in the East, but the stress regime is extensive except for the Orsova area where σ1 is EW oriented in a compressive regime [8]. In CSCSZ, the stress regime changes from transtensive in Hateg Basin to compressive between Petrosani and Tg. Jiu (transcurrent and inverse faults) and σ1 rotates from NV–SE to NE–SW. σ1 changes its orientation from NE–SW to E–V and then NV–SE also in FCSZ, in an extensive stress regime.

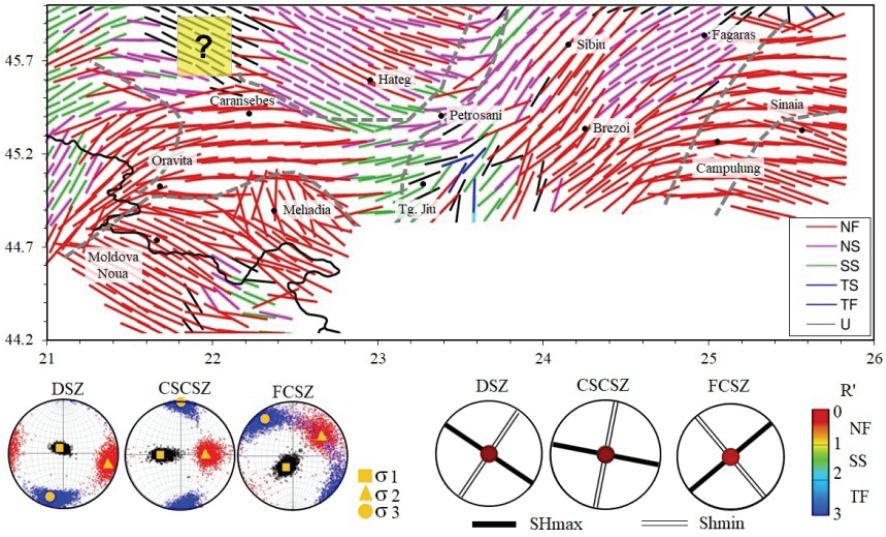

Fig. 4 – (Color online) Formal inversion of focal mechanisms; top: orientation of the σ1 axis of the stress tensor (coloured lines), the colours correspond to the type of fault: NF, normal; NS, normal-transcurrent oblique; SS, transcurrent (strike-slip); TF, reverse-transcurrent oblique; TF, inverse; U, uncertain; the grey dotted lines delimit homogeneous sectors of the stress field (the same orientation of the σ1 axis); bottom: pie charts for seismogenic areas: stress tensor (left) and horizontal stress axes Shmax and Shmin (right); the full-coloured circle in the middle of the diagram symbolizes the stress regime.

In Table 4 are presented the seismotectonic characteristics in numerical format (reactivation potential, ST, Mmax, recurrence parameters and Tr) for the main seismogenic structures. For example, in the Mehadia active zone were 2 earthquakes with Mw ≥ 5.0 (11.10.1910, Mw = 5.2; 18.07.1991, Mw = 5.7) are known the faults with the highest probability of reactivation (95%) are oriented on average EV (North of Mehadia and at the intersection FV-FCJ-FZLO), while faults with orientation from NNV–SSE to NE–SV have 75–80% probability of reactivation. Reactivation is predominantly as transcurrent faults with the normal component or normal faults. Here, an earthquake with Mwmax = 6.2 (maximum observed Mw + 0.5 u.m) is Tr ≈ 1300 years, and an earthquake with M = 5.7 occurs once every 460 years.

The nodal planes of the focal mechanism of the earthquake of 18.07.1991 (Mw = 5.7) suggest that the FMI, oriented E–V is most likely the causal fault. In the Moldova Noua-Oravita area, the faults oriented on average ESE–VNV can be reactivated as normal or transcurent faults. The focal mechanism of the earthquake of 24.05.2002 in Moldova Noua and the study of [42] show that the WNW-ESE (FNSMN) oriented faults have been reactivated.

An earthquake with Mw = 5.5 has, in these conditions, Tr ≈ 70 years, and earthquakes with Mmax = 6.2 can occur once every 200 years. In FCSZ the NNE-SSV to NE–SV faults (FOltului, FVSt) and ENE–VSV (FCozia) are the most vulnerable in the contemporary active stress field. In the Campulung area, FIM (oriented NV–SE), FCozia (oriented E–V) and the FCO-SHo system (oriented NNE-SSV) can be reactivated either as normal or pure transcurrent faults or with a normal component. The strong earthquakes associated with these faults (Mw = 6.4) have Tr ≈ 300 years.

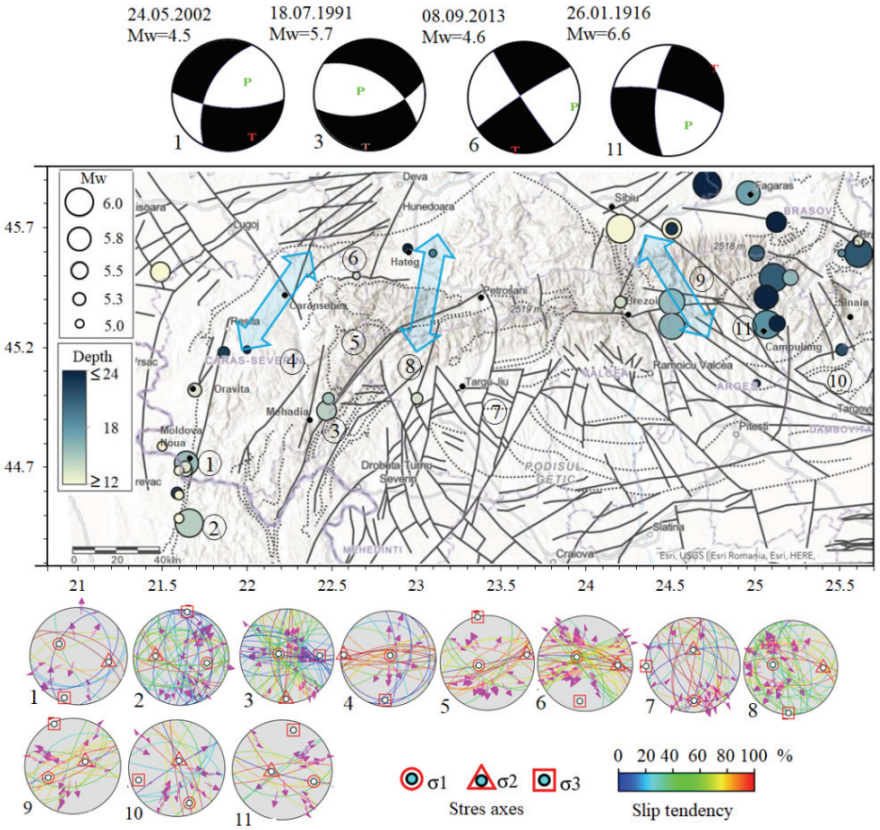

Fig. 5 – (Color online) Seismotectonic characteristics. top: focal mechanisms for earthquakes representative of active seismic areas; middle: seismotectonic sketch; blue arrows = Shmin, down: stereograms of the fault planes (lower hemisphere Wulff) and their tendency to slide in percentage; the red arrows show the direction of movement on the fault.

The focal mechanism of the earthquake of 26.01.1916 (Mw = 6.6) shows that, at least in the Eastern extremity of the FCSZ area and at a depth h > 20 km, the compression (P axis) is on the NW–SE direction similar to that of the curvature of the Carpathians [25]. In the NW part of the CSCSZ, the fault systems from the Hateg Basin oriented ENE–VSV and VNV–ESE and the ENE–VSV fault system oriented from the Retezat-Godeanu Block, parallel to the Cerna-Jiu Fault, can be reactivated with a high probability as transcurrent or normal faults. The faults in the Timok-Baia de Arama and SDM system and the N–S oriented faults in the FTgJCa system have maximum reactivation potential as normal and transcurrent faults, respectively. The recurrence period for a major earthquake in this area (Mwmax = 5.7) is Tr = 988 years.

5. CONCLUSIONS

Our paper brings new data for knowing and understanding the seismotectonic processes in the South Carpathians. The seismogenic potential of the seismically active geological structures and the recurrence periods for the observed and possible maximum magnitudes were numerically evaluated.

The earthquakes catalogue used in this study has a high level of homogeneity and accuracy (location parameters, magnitude), is based on instrumental and macroseismic data revised or obtained for the primary sources (seismograms, bulletins). Macroseismic parameterization was performed using recently instrumentally calibrated methods. Our catalogue contains 132 new earthquakes and removes a series of false earthquakes from the Romplus catalogue. Major earthquakes (Mw > 5) are associated with stressed geological structures (b-value < 0.8) and asperities with a high potential for future reactivation. Under the seismotectonic conditions described in this study, strong earthquakes with Mmax may occur in the future, possibly about 200 years in the western region (DSZ) or about 580 years in the east (FCSZ).

The focal mechanism determined for the strong earthquake of 26.01.1916 in the Fagaras-Campulung area suggests the strong influence of the stress field characteristic of the curvature area of the Romanian Carpathians, especially in the lower part of the lithosphere (h > 20 km).

Acknowledgements. This paper was carried out within Nucleu Program MULTIRISC supported by MCI, projects number PN19080101 and PN19080102 and Phenomenal Project PN-III-P2-2.1-PED-2019-1693, 480PED/2020 supported by UEFISCDI.

REFERENCES

1. M. Radulian, N. Mandrescu, G.F. Panza, E. Popescu and A. Utale, *Characterization of Seismogenic Zones of Romania*, Pure and Applied Geophysics **157**, 57–77 (2000).
2. C. Ghita, M. Diaconesu, I. A. Moldovan, E. Oros, and E. G. Constantinescu, *Spatial and temporal variation of seismic b-value beneath Danubian and Hateg-Strei seismogenic areas*, Romanian Reports in Physics **72**, 704 (2020).

3. E. Oros, *Cercetari privind hazardul seismic pentru Regiunea Seismica Banat*, Teza de doctorat, Univesitatea Bucuresti, Fac. De Fizica (2011).
4. A. O. Placinta, E. Popescu, F. Borleanu, M. Radulian and M. Popa, *Analysis of source properties for the earthquake sequences in the South-Western Carpathians (Romania)*. Romanian Reports in Physics **68**, 1240–1258 (2016).
5. M. Popa, I. Munteanu, F. Borleanu, E. Oros, M. Radulian and C. Dinu, *Active tectonic deformation and associated earthquakes: a case study – South West Carpathians Bend zone,* Acta Geodaetica et Geophysica **53**, 395–413 (2018).
6. A. Bala, M. Radulian and D. Toma-Danila, *Crustal stress partitioning in the complex seismic active areas of Romania*, Acta Geodaetica et Geophysica **55**, 389–403 (2020).
7. E. Oros, M. Popa, M. Diaconescu and M. Radulian, *Active stress field and seismotectonic features in Intra-Carpathian region of Romania,* EGU General Assembly 2017, 23–28 April 2017, Viena, Austria, Geophysical Research Abstracts, Vol. **19**, EGU2017-13103 (2017).
8. E. Oros, A.O. Placinta and I.A. Moldovan, *The analysis of earthquakes sequence generated in the Southern Carpathians, Orsova June-July 2020 (Romania): seismotectonic implications*, Romanian Reports in Physics **73**, 706 (2021).
9. E. Oros, M. Popa, D. Paulescu, A.O. Placinta and C. Ghita, *A refined catalogue of focal mechanisms for the Intra-Carpathian region of Romania: implications for the stress field and seismogenic features assessment*, Annals of Geophysics (in press) (2020a).
10. V. Răileanu, C. Dinu, L. Ardeleanu, V. Diaconescu, E. Popescu and A. Bălă, *Crustal seismicity and associated fault systems in Romania*, Proceedings of the 27th ECGS Workshop: Seismicity Patterns in the Euro-Med Region, Luxembourg, 17–19 Nov. 2008, in "Cahiers du Centre Europeen de Geodynamique et de Seismologie", 153–159 (2009).
11. M. Sandulescu (1984), *Geotectonica României*, Editura Tehnica, Bucuresti (1984).
12. I. Stelea, *Comments on the supragetic nappe in the central-eastern south Carpathians,* Muzeul Olteniei Craiova, Studii şi comunicări, Ştiinţele Naturii, Tom. **32**, No. 1/2016, 7–11 (2016).
13. M. C. Oncescu, V. Marza, M. Rizescu and M. Popa, *The Romanian Earthquake Catalogue Between 984 – 1997*, In: Wenzel F., Lungu D., Novak O. (eds) Vrancea Earthquakes: Tectonics, Hazard and Risk Mitigation. Advances in Natural and Technological Hazards Research, Springer, Dordrecht, **11**, 43–47 (1999).
14. E. Oros, M. Popa and I.A. Moldovan, *Seismological DataBase for Banat Seismic Region (Romania) – Part 1: The Parametric Earthquake Catalogue*. Rom. Journ. Phys, **53** 7–8. 955–964 (2008).
15. L. Matenco, G. Bertotti, S. Cloetingh and C. Dinu., S*ubsidence analysis and tectonic evolution of the external Carpathian–Moesian Platform region during Neogene*, Sedimentary Geology, **156**, 71–94 (2003).
16. H. Savu, *Exhumation of the South Carpathians (Romania) and their block structure*, Romanian Journal of Earth Sciences, **86**, 1, 51–58 (2012).
17. L. Matenco, K. Csaba, S. Merten, S. Stefan, S. Cloetingh and P. Andriessen, *Characteristics of collisional orogens with low topographic build-up: example Carpathians*, Terra Nova, **22/3**, 155–165 (2010).
18. M. Nemčok, G. Pogácsás and L. Pospisil, *Activity Timing of the Main Tectonic Systems in the Carpathian–Pannonian Region in Relation to the Rollback Destruction of the Lithosphere*, In: The Carpathians and Their Foreland: Geology and Hydrocarbon Resources (J. Golonka, F. J. Picha edits) (2006).
19. H.G. Linzer, W. Frisch, P. Zweigel, R. Girbacea, H.P. Hann and F. Moser, *Kinematic evolution of the Romanian Carpathians*, Tectonophysics **297** (1– 4), 133– 156 (1998).
20. E. Oros, M. Popa, C. Ghita, M. Rogozea, A. Rau-Vanciu and C. Neagoe, *Catalogue of focal mechanism solutions for crustal earthquakes in Intra-Carpathian region of Romania*. 35th General Assembly of the European Seismological Commission. 4–11 Sept. 2016, Trieste, Italy, ESC2016-142 (2016).
21. B. Glavatovic and S. Akkar, NATO SfP Project 983054, *Harmonization of Seismic Hazard Maps for the Western Balkan Countries (BSHAP)*, Final Report, AB38745 (2011).

22. F. Horvath, G. Bada, P. Szafian, G. Tari, A. Adam and S. Cloetingh, *Formation and deformation of the Pannonian Basin: constraints from observational data*, In: Gee, Stephensen, (Eds.), European Lithosphere Dynamics. Geol. Soc. of London, 191–206 (2006).
23. I. Joo, *Recent vertical surface movements in the Carpathian Basin*, Tectonophys. **202**, 129–134 (1992).
24. G. Polonic, D. Zugrăvescu and I. Toma, *Dinamica recentă a blocurilor tectonice în zonele de amplasament al construcţiilor hidroenergetice din România*, St. Cerc. Geofizică, **43**, 79–93 (2005).
25. D. Zugrăvescu, G. Polonic, M. Horomnea and V. Dragomir, *The crustal vertical recent movements on the Romanian Territory, the major tectonic compartments and their relative dynamics*, Revue Roum. Géophysique, **42**, 3–14 (1998).
26. J. Havskov, P.H. Voss and L. Ottemoller, *Seismological Observatory Software: 30 Yrs of SEISAN*, Seismological Research Letters (2020) **91** (3): 1846–1852 (2020).
27. E. Oros, M. Popa and M. Rogozea, *Calibration of crustal historical earthquakes from the Intra-Carpathian region of Romania*, WMESS 2017 Conference Proceedings, IOP Publishing Earth and Environmental Science, 032004, doi:10.1088/1755-1315/95/3/032004 (2017a).
28. F. Bernardi, J. Braunmiller and D. Giardini, *Seismic Moment from Regional Surface-Wave Amplitudes*, Bulletin of the Seismological Society of America, **95**, 2, 408–418 (2005).
29. E. Oros, A.O. Placintă and M. Popa, *Calibration and validation of MEEP method for location and magnitude estimation of historical earthquakes from Intra-Carpathian region of Romania*, WMESS 2017 Conference Proceedings, IOP Publishing Earth and Environmental Science, vol. **221,** DOI: 10.1088/1755-1315/221/1/012057 (2019).
30. E. Oros, A.O. Placinta, M. Popa, M. Rogozea and D. Paulescu, *Attenuation of macroseismic intensity for crustal Romanian earthquakes: calibrating the Bakun-Wentworth's method.* WMESS 2019 Conference Proceedings, IOP Conference Series Earth and Environmental Science, vol. **362**, DOI:10.1088/1755-1315/362/1/012026 (2019a).
31. M.W. Musson and M.J. Jimenez, *Macroseismic estimation of earthquake parameters, NERIES project report*, Module **NA4**, Deliverable D3 (Edinburgh) (2008).
32. W.H. Bakun and C.M. Wentworth*, Estimating earthquake location and magnitude from Seismic Intensity Data*, Bulletin of Seismological Society of America, **87**, 6, 1502 – 1521 (1997).
33. T. Zsiros, *A Karpatmedence szeismicitasa es foldrenges esyelzessege: Magyar forldrenges katalogus (456-1995)*, GGRI, Hungarian Academy of Sciences (2000).
34. J.L. Hardebeck and P.M. Shearer, *A new method for determining first-motion focal mechanisms*, Bulletin of Seismological Society of America, **92**, 2264–2276 (2002).
35. J.L. Hardebeck and P.M. Shearer, *Using S/P amplitude ratios to constrain the focal mechanisms of small earthquakes*, Bulletin of Seismological Society of America, **93**, 2434–2444 (2003).
36. S. Wiemer, *A software package to analyze seismicity: ZMAP*, Seismological Research Letter, **92**, 373–382 (2001).
37. C.H Scholz, *On the stress dependence of the earthquake b-value*, Geophysical Research Letters, **42**, 1399–1402 (2015).
38. D. Delvaux and B. Sperner, *Stress tensor inversion from fault kinematic indicators and focal mechanism data: the TENSOR program*, In New Insights into Structural Interpretation and Modelling (D. Nieuwland Editor), Geol. Society, London, Spec. Publications, **212**, 75–100 (2003).
39. A. Morris, D.A. Ferrill and D.B. Henderson, *Slip-tendency analysis and fault reactivation,* Geology, **24** (3): 275–278 (1996).
40. E. Oros, D. Paulescu and M. Popa, *The M6.4, 26th January 1916 earthquake under review: new data on the seismicity of Fagaras Seismogenic Region (Romania),* Proceedings, 31st General Assembly of the European Seismological Commission ESC 2008, Crete, 7–12 September 2008 (2008b).
41. E. Oros, E. Constantinescu, D. Paulescu, M. Popa and A.O. Placinta, *Using early instrumental data to determine the source parameters of the strongest historical earthquakes that occurred in west Romania (1900–1980),* Proceedings SGEM 2019, Vol. **19**, Science and Technologies in Geology, Exploration and Mining, Issue: 1.1, pp. 991–99, DOI: 10.5593/sgem2019/1.1/S05.122 (2019b).
42. E. Oros, The April–August Moldova Noua earthquakes sequence and its seismotectonic significance, Revue Roumaine de Geophysique, **48**, 49–68 (2004).